# Inelastic $\alpha$ scattering from $^{20}$Ne

C. A. Davis*
*University of Wisconsin, Madison, Wisconsin 53706*
(Received 29 January 1992)

Cross sections for $^{20}$Ne$(\alpha,\alpha_{1,2,3})$ were measured from $E_\alpha=5.6$ ($\alpha_1$), 7.5 ($\alpha_2$), and 9.5 ($\alpha_3$) MeV up to 11.0 MeV in steps of 10 and 15 keV at up to 20 angles. The $\alpha_1$ data were fitted with a Legendre polynominal expansion, thus allowing limits to be placed on the spin and parity of 31 levels in $^{24}$Mg, about five of which have not previously been seen in elastic $\alpha$ scattering. In the $\alpha_2$ data some 15 levels are identified as to energy and width.

PACS number(s): 25.55.Ci, 27.30.+t

## I. INTRODUCTION

An analysis of elastic alpha scattering from $^{20}$Ne [1] has revealed an extensive series of natural parity states in the compound nucleus, $^{24}$Mg. Many of these states, as well as many others, have been summarized in Ref. [2]. In this paper, we report data on the inelastic scattering of alphas from $^{20}$Ne, which, for the most part, were obtained from the same spectra upon which the data reported in Ref. [1] were based. We refer the readers to Ref. [1] for a description of the experiment and data reduction. The present work reports excitation functions of inelastic scattering of alphas from $^{20}$Ne, to the first excited state (1.634 MeV, $2^+$) from $E_x(^{24}\text{Mg})=14.0$ to 18.5 MeV, at a sufficient number of angles that a Legendre polynomial fit was done to the data; to the second excited state of $^{20}$Ne(4.248 MeV, $4^+$) from $E_x(^{24}\text{Mg})=15.5$ to 18.5 MeV at only a very few angles; and to the third excited state of $^{20}$Ne (4.970 MeV, $2^-$) from $E_x(^{24}\text{Mg})=17.2$ to 18.5 MeV. Previous work [3] has provided excitation functions, at two laboratory angles only, for these states, from $E_x(^{24}\text{Mg})=20.3$ to 26.5 MeV.

About 11 000 cross sections in the three inelastic channels were measured. As the rather extensive data set can only be presented in a qualitative way in the present work, we have deposited the 117 pages of differential cross sections and Legendre fits with the AIP Physics Auxiliary Publication Service [4].

## II. INELASTIC SCATTERING TO THE FIRST EXCITED STATE OF $^{20}$Ne

The differential cross sections for the $^{20}$Ne$(\alpha,\alpha_1)^{20}$Ne(1.634 MeV, $2^+$) reaction were measured in the range 5.6 MeV $\leq E_\alpha \leq$ 11.0 MeV in steps of 10 and 15 keV. Excitation functions at selected angles are presented in Fig. 1. In the initial data set, as used to provide information about the $^{20}$Ne$(\alpha,\alpha_0)^{20}$Ne(g.s) reaction [1], there were no more than sixteen angles for each angular distribution. This presented a problem in fitting, especially as there were no data forward of $\theta_{\text{lab}}=45°$. Additional data were measured over the energy region $5.6 \leq E_\alpha \leq 10.6$ MeV, especially at forward angles along with data at angles identical to several angles in the original data set to establish a common normalization. The second data set was then used to interpolate data (using a polynomial interpolation from the nearest neighbor data at each angle) at the additional angles for the original data set (as the original data set was of varying step size), providing a total of up to twenty angles at each energy. This set was also used as a separate energy calibration to which the original data sets were adjusted as it was measured across the whole energy range at one time as opposed to several subsets with slightly different target thicknesses; thus, the present work provides an independent determination of resonance energies from the values derived from the elastic scattering data [1]. This difference in energy calibration varies from about 17 keV above to 1 keV below the $\alpha_0$ calibration, and should be remembered when comparing resonant energies from the $(\alpha,\alpha_0)$ and $(\alpha,\alpha_1)$ channels. Despite the fact that the additional data were of lower counting statistics and included an error for the interpolation process, so that the total errors for these angles are significantly larger than the errors of the original data, they constrain the fits from producing unphysical results (i.e., negative cross section) at the forward angles.

As stated in Ref. [1], the energy uncertainty arises principally from the uncertainty in the beam-energy calibration and, especially, poor knowledge of the pressure profile and He/Ne mixture at the beam entrance collimator, and was estimated to be $\sim$10 keV or a little worse. On average, the inelastic resonant energies agree with the elastic channel energies (for those resonances for which the widths are in approximate agreement and the spin assignments are consistent) to within an average variance of about 20 keV. As the estimates of the resonance energy may be influenced by the interference between the resonance partial waves and the background, errors of the order of the resonance width should be expected. The uncertainties in cross sections principally depend on uncertainty in the laboratory scattering angle, the errors in the

*Permanent address: TRIUMF, 4004 Wesbrook Mall, Vancouver, B.C., Canada V6T 2A3; and University of Manitoba, Department of Physics, Winnipeg, Manitoba, Canada R3T 2N2.

 

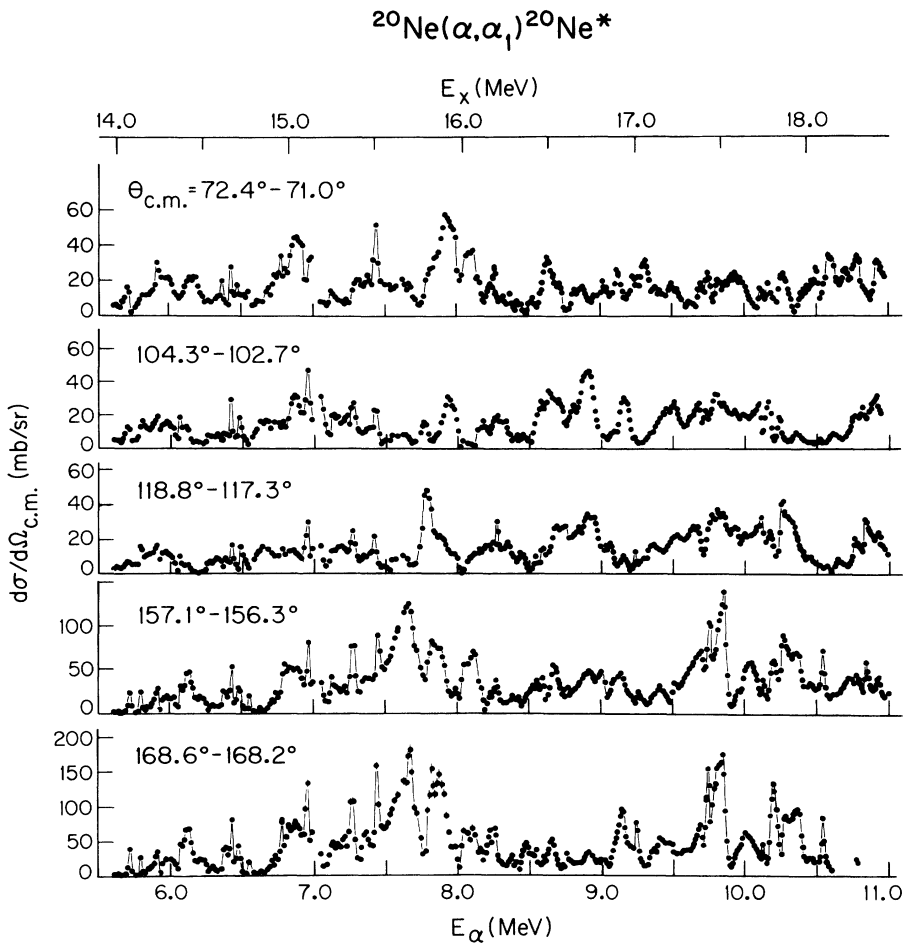


FIG. 1. Excitation functions at selected angles for inelastic $\alpha$ scattering to the first excited state of $^{20}$Ne. The line segments are a guide to the eye in regions of sharp structure.

acceptance for each detector telescope, errors in measurement of the gas pressure in the target chamber along with beam heating effects in the gas, and errors in measurement of the integrated beam current which, together, were about 2–3 % [5], dependent upon the scattering angle.

The $^{20}Ne(\alpha,\alpha_1)^{20}Ne^*(1.63\ \text{MeV}, 2^+)$ angular distributions were expanded in terms of Legendre polynomials:

$$\frac{d\sigma}{d\Omega} = \sum_{\nu=0}^{2L} a_\nu P_\nu(\cos\theta) \ . \tag{1}$$

This gives the total cross section, $\sigma_T = 4\pi a_0$, and the highest order Legendre polynomial required which depends on the angular momentum. The $a_\nu$ were determined by the linear least-squares fit by Eq. (1) for a particular maximum order of Legendre polynomial $\nu_{max} = 2L$. The value of $\nu_{max}$ was determined by the fact that increasing it would no longer improve the $\chi^2$ per degree of freedom. The $\chi^2$ per degree of freedom were quite good below about $E_x = 16$ MeV. Above $E_x = 16$ MeV the lack of data at angles smaller than $\theta_{c.m.} = 30°$ made it necessary to constrain the fits from becoming negative at forward angles, as was done in Ref. [5]. This means that the fit forward of 30° is inaccurate and the errors of $a_\nu$ become larger. Several fits to angular distributions are presented in Fig. 2. The values of $a_\nu$ as a function of energy are presented in Fig. 3–6, the total cross section being given at the top of Figs. 3 and 5. There were insufficient angular data to achieve useful fits from $10.6 \le E_\alpha \le 11.0$ MeV.

The Legendre fits set limits on the spin of states excited in the compound nucleus. The reaction has the spin structure $0^+ + 0^+ \rightarrow 0^+ + 2^+$. If, at some energy, the incoming orbital angular momentum $l$ excites a resonance, then the spin and parity of that resonance are $J = l$, $\pi = (-)^l$. The outgoing orbital angular momenta $l'$ are confined to the range $|l-2| \le l' \le l+2$ and conserve parity. It has been shown [6,7] that $L$ may not exceed the minimum of $l$, $J$, or $l'$. The possibilities of $J^\pi$ for a given $L$ in this channel are presented in Table I.

Several resonances were identified (see Table I) and the values for the resonant parameters were estimated. In most cases the value $L = \nu_{max}/2$ was unambiguous, though sometimes $\nu_{max}$ was odd, possibly from interference of a resonance with $L = (\nu_{max}-1)/2$ and an otherwise insignificant $L+1 = (\nu_{max}+1)/2$ background strength. However, if this odd $\nu_{max}$ was significant, then

TABLE I. Resonances in $^{24}$Mg deduced from $^{20}$Ne$(\alpha,\alpha_1)^{20}$Ne* excitation functions and Legendre polynomial fits to same, and from $^{20}$Ne$(\alpha,\alpha_2)^{20}$Ne*, compared to resonances observed in elastic α scattering from $^{20}$Ne in Ref. [1]. An asterisk indicates a possible doublet as reported in Ref. [1].

| $(\alpha,\alpha_1)$ resonances | | | | | $(\alpha,\alpha_2)$ resonances | | | $(\alpha,\alpha_0)$ resonances[a] | | |
|---|---|---|---|---|---|---|---|---|---|---|
| $E_\alpha$ (MeV) | $E_x$ (MeV) | $L$ | $J^\pi$ | $\Gamma_{c.m.}$ (keV) | $E_\alpha$ (MeV) | $E_x$ (MeV) | $\Gamma_{c.m.}$ (keV) | $E_x$ (MeV) | $J^\pi$ | $\Gamma_{c.m.}$ (keV) |
| 5.715 | 14.072 | 2 | $2^+,4^+$ | 21 | | | | (14.070) | (odd) | ~17 |
| | | | | | | | | 14.076[b] | | 24±5 |
| | | | | | | | | (14.090) | | ~21 |
| | | | | | | | | 14.10[c] | $(2,4)^+$ | |
| 5.790 | 14.134 | 2 | $2^+,4^+$ | ≤13 | | | | 14.145[c] | $4^+(3^-,5^-)$ | |
| | | | | | | | | 14.146[d] | $(3^-,4^+,5^-)$ | 1.8±0.4 |
| | | | | | | | | 14.148[b] | | 6.2±0.7 |
| | | | | | | | | 14.158 | $4^+$ | 11.2±1.9 |
| 5.915 | 14.238 | 2 | $2^+,4^+$ | ≤ 13 | | | | 14.241[b] | | 11.3±1.4 |
| | | | | | | | | 14.257 | $4^+$ | 16±2 |
| 6.01 | 14.32 | (0,1) | $(0^+2^+,1^-3^-)$ | ~167 | | | | 14.348 | $(3^-)$ | 112±29 |
| 6.063 | 14.362 | 2 | $2^+,4^+$ | ≤ 13 | | | | 14.390 | $4^+$ | 12±3 |
| 6.138 | 14.424 | 2 | $2^+,4^+$ | 42 | | | | 14.454 | $4^+$ | 46 |
| 6.350 | 14.601 | (3) | $(3^-,5^-)$ | ≤13 | | | | 14.562 | odd (not 3) | ≤13 |
| 6.423 | 14.661 | 4 | $4^+,6^+$ | ≤15 | | | | 14.641 | $6^+$ | 11±9 |
| 6.475 | 14.705 | 3 | $3^-,5^-$ | 21 | | | | 14.689 | $5^-$ | 9±1 |
| 6.54 | 14.76 | (1,2) | $(1^-3^-,2^+4^+)$ | ≤21 | | | | 14.738 | $4^+$ | 13 |
| | | | | | | | | 14.81[e] | $1^-$ | |
| 6.793 | 14.970 | 3 | $3^-,5^-$ | ≤13 | | | | 14.988 | $(4^+,5^-)$ | ~20 |
| 6.958 | 15.107 | (3,4) | $(3^-5^-,4^+6^+)$ | ≤13 | | | | 15.110 | $4^+$ | 15 |
| | | | | | | | | 15.134 | $4^+$ | 15 |
| 7.080 | 15.209 | 3(4) | $3^-,5^-(4^+,6^+)$ | 33 | | | | 15.207 | $5^-$ | 36±3 |
| 7.267 | 15.365 | 2(3) | $2^+,4^+(3^-,5^-)$ | 25 | | | | 15.347 | $4^+$ | 21±4 |
| | | | | | | | | 15.378 | $4^+$ | 31±7 |
| 7.440 | 15.510 | (5,6) | $(5^-7^-,6^+8^+)$ | 21 | | | | 15.526 | $6^+$ | 18±2 |
| 7.65 | 15.68 | (3,4) | $(3^-5^-,4^+6^+)$ | 21 | 7.650 | 15.684 | 13 | 15.68 | $(0^+)$ | ≤15 |
| | | | | | | | | 15.71 | $(4^+)$ | ≤25 |
| 7.76 | 15.78 | 2 | $2^+,4^+$ | 33 | | | | 15.786 | $4^+$ | 13 |
| | | | | | 7.815 | 15.821 | 21 | 15.821 | odd | 87 |
| | | | | | | | | 15.846 | | <13 |
| 8.00 | 15.98 | 1 | $1^-,3^-$ | 21 | 7.995 | 15.971 | ≤13 | 15.971 | odd | ~35 |
| | | | | | | | | (15.971) | (even) | narrow |
| 8.25 | 16.18 | 4 | $4^+,6^+$ | ≤13 | | | | 16.162 | | <8 |
| | | | | | | | | 16.196 | $6^+$ | 8 |
| 8.42 | 16.32 | 4 | $4^+,6^+$ | ≤8 | | | | (16.32) | | narrow |
| | | | | | 8.570 | 16.450 | 21 | 16.433 | $7^-$ | 10 |
| 8.582 | 16.460 | (4) | $(4^+,6^+)$ | ≤17 | | | | 16.470 | $6^+$ | 8±2 |
| 8.652 | 16.518 | 4 | $4^+,6^+$ | ~33 | | | | 16.521 | $6^+$ | 31 |
| 8.699 | 16.557 | 4(5) | $4^+,6^+(5^-,7^-)$ | ~33 | | | | 16.597 | $4^+$ | 30 |
| | | | | | 8.800 | 16.641 | 17 | 16.666 | (even)* | 30 |
| | | | | | | | | (16.73) | (odd) | ≤8 |
| | | | | | 8.962 | 16.776 | 33 | 16.775 | $(4^+,6^+)$* | 30 |
| 9.034 | 16.836 | (3,4) | $(3^-5^-,4^+6^+)$ | ≤8 | | | | 16.837 | $(6^+)$* | 22 |
| | | | | | 9.115 | 16.904 | 42 | 16.922 | $6^+$ | 44±6 |
| 9.134 | 16.920 | (4,5) | $(4^+6^+,5^-7^-)$ | ≤8 | | | | | | |
| 9.24 | 17.01 | 4 | $4^+,6^+$ | ≤8 | | | | 17.010 | $7^-$ | 15±10 |
| 9.34 | 17.09 | (5) | $(5^-,7^-)$ | ~42 | 9.31 | 17.07 | 37 | 17.080 | $6^+$ | 44±6 |
| | | | | | | | | 17.133 | $5^-$ | 26±6 |
| | | | | | 9.732 | 17.418 | 13 | 17.399 | $6^+$ | 20 |
| 9.78 | 17.46 | 5(6) | $5^-,7^-(6^+,8^+)$ | ≤8 | | | | | | |
| | | | | | 9.826 | 17.496 | 29 | 17.437 | $6^+$ | 20 |
| | | | | | | | | (17.47) | (even) | |
| | | | | | 9.95 | 17.60 | 13 | 17.615 | $5^-$ | 23±8 |
| 10.11 | 17.73 | (4,5) | $(4^+6^+,5^-7^-)$ | ≤8 | | | | 17.73 | $4^+$ | ~25 |

TABLE I. (*Continued*).

| $(\alpha,\alpha_1)$ resonances | | | | | $(\alpha,\alpha_2)$ resonances | | | $(\alpha\alpha_0)$ resonances[a] | | |
|---|---|---|---|---|---|---|---|---|---|---|
| $E_\alpha$ (MeV) | $E_x$ (MeV) | $L$ | $J^\pi$ | $\Gamma_{c.m.}$ (keV) | $E_\alpha$ (MeV) | $E_x$ (MeV) | $\Gamma_{c.m.}$ (keV) | $E_x$ (MeV) | $J^\pi$ | $\Gamma_{c.m.}$ (kev) |
| 10.190 | 17.799 | 4(5) | $4^+,6^+(5^-,7^-)$ | 21 | 10.205 | 17.812 | 25 | 17.77 | (not $4^+$) | ~42 |
| | | | | | | | | 17.83 | (not $4^+$) | ~42 |
| | | | | | 10.512 | 18.067 | ≤8 | | | |
| 10.530 | 18.082 | 4(5) | $4^+,6^+(5^-,7^-)$ | 33 | | | | 18.089 | * | 20 |
| | | | | | 10.605 | 18.145 | 33 | 18.149 | $5^-$ | 20 |
| | | | | | 10.750 | 18.266 | 25 | 18.27 | $7^-$ | ~21 |

[a] From Ref. [1] except where noted.
[b] $^{20}$Ne$(\alpha,\alpha'\gamma)^{20}$Ne from Ref. [11].
[c] $^{20}$Ne$(\alpha,\gamma)$ from Ref. [12].
[d] $^{20}$Ne$(\alpha,\gamma)$ from Ref. [11].
[e] $^{20}$Ne$(\alpha,\gamma_0)^{24}$Mg from Ref. [10].

the next higher $L$ is listed in parentheses, following the lower $L$, in Table I. The interpolation process for the forward angle data also tends to smooth out the effects of narrower structure at these forward angles, and hence contributes to the difficulty of recognizing the appropri-

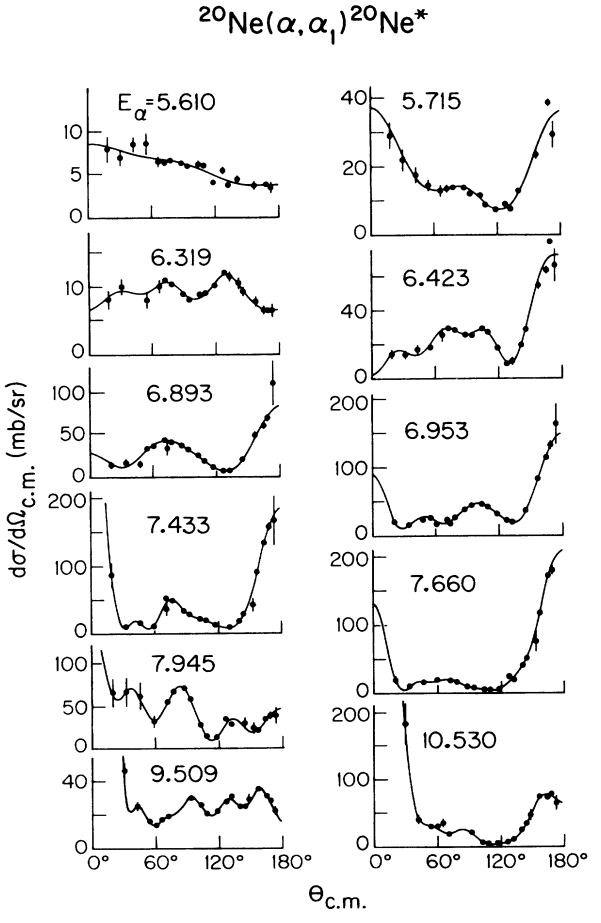


FIG. 2. Selected angular distributions at selected energies for the $^{20}$Ne $(\alpha,\alpha_1)^{20}$Ne* reaction. The solid lines represent the Legendre polynomial fit to each angular distribution. The energies are in MeV.

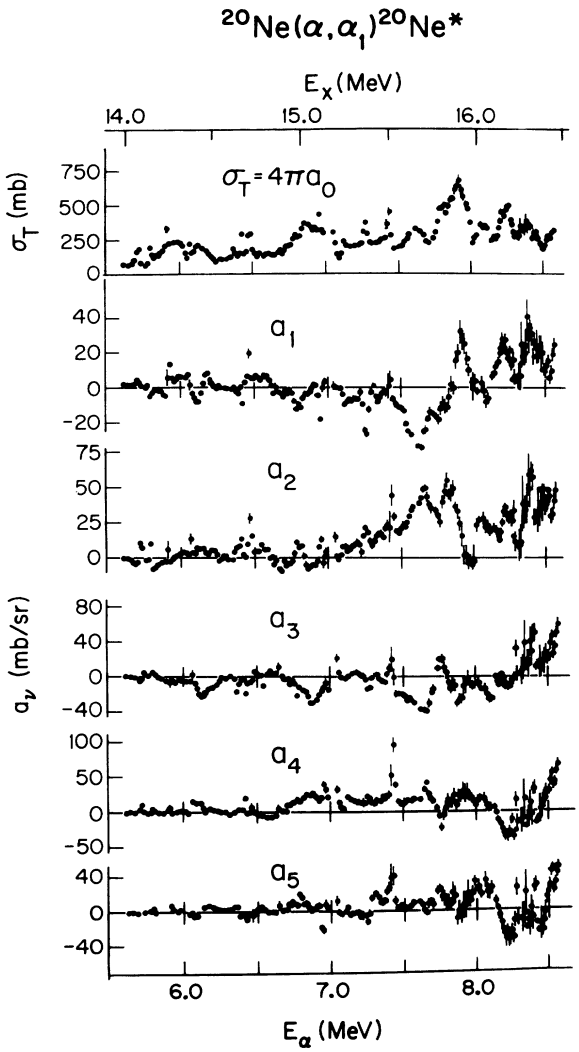


FIG. 3. The results of the Legendre polynomial fit for the data at $E_x$ below 16.5 MeV and for $\nu=0$ through 5. The total cross section ($\sigma_T=4\pi a_0$) is at the top.

ate $\nu_{max}$. Thus, in some cases, the $L$ is uncertain or there is more than one possibility for $L$ and this is indicated by parentheses in the $L$ column of Table I. Once $L$ is known, then limits are placed on $J^{\pi}$. Some of the resonances for which there is evidence of previous observation in Ref. [1] or elsewhere are discussed below.

## III. INELASTIC SCATTERING TO THE SECOND AND THIRD EXCITED STATES OF $^{20}$Ne

Figure 7 shows data at several sample angles for the $^{20}$Ne$(\alpha,\alpha_2)^{20}$Ne* reaction, but I had an insufficient number of angles for a satisfactory Legendre fit. However, some estimates for $E_\alpha$ and $\Gamma$ were made by visual inspection of the data, and these values are also listed in Table I. Figure 8 shows a few unfitted angular distributions for this inelastic channel.

A small amount of data (not shown here, but included in the AIP PAPS file, Ref. [4]) was also obtained for the $^{20}$Ne$(\alpha,\alpha_3)^{20}$Ne* reaction. Background made it very difficult to reduce these data and there is some bad overlap between data sets.

## IV. DISCUSSION OF THE RESONANCES

For most of the resonances for which a definite $J^{\pi}$ assignment is made in the $(\alpha,\alpha_0)$ and a definite $L$ assignment is made in the $(\alpha,\alpha_1)$ channels, the agreement is with the higher $J$ value deduced from the $L$ in the Legendre fit to the $(\alpha,\alpha_1)$ data. The higher $J$ corresponds to an outgoing orbital angular momentum of $l'=L$, whereas the lower $J$ corresponds to $l'=L+2$; thus the higher angular momentum associated with the lower $J$ has a higher centripetal barrier for the outgoing $\alpha$. While the barrier penetration factors for the incident alpha angular momenta ($l$) behave in a contrary way for the two $J$'s, this is less important as it is at higher energy.

The state at $E_\alpha=9.034$ MeV corresponds to structure that was reported as a possible doublet, one member of which was probably at $6^+$, consistent with the $L=(3,4)$ assignment in the present work. There are also three narrow ($\Gamma_{c.m.}\leq 8$ keV) $(\alpha,\alpha_1)$ resonances at $E_\alpha=9.134$, 9.24, and 9.78 MeV which do not agree in width or spin with

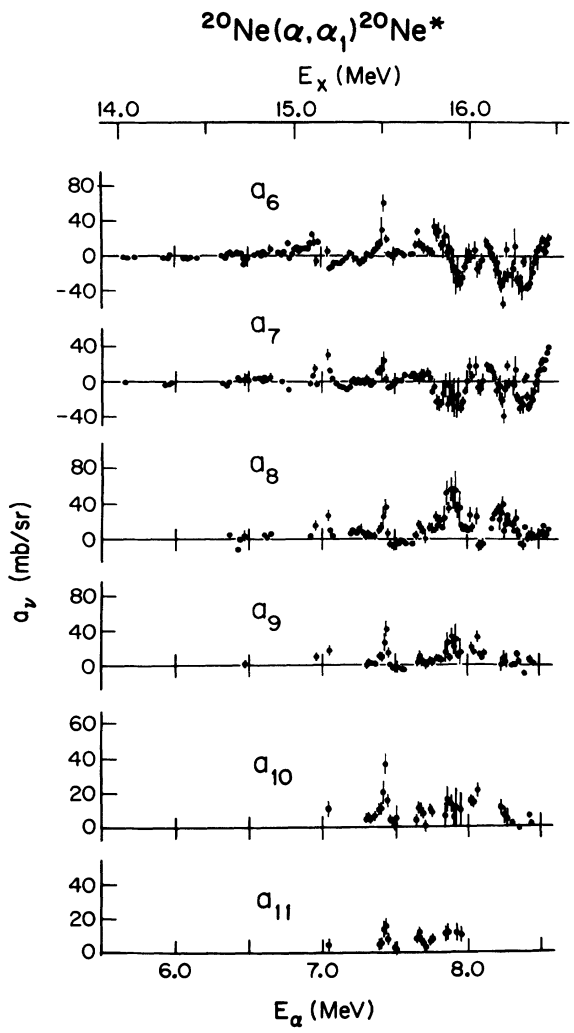


FIG. 4. As in Fig. 3 for the Legendre coefficients $\nu=6$ through 11.

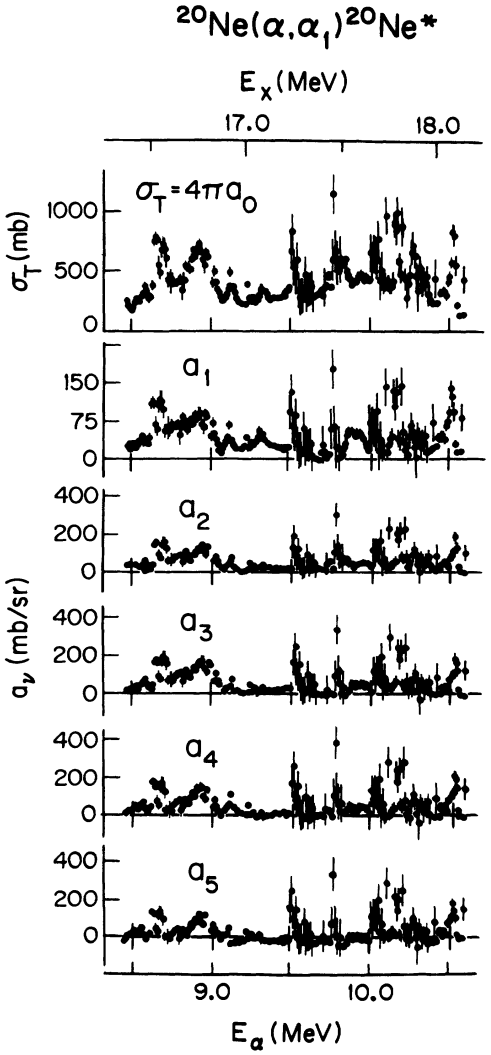


FIG. 5. As in Fig. 3 for $E_x>16.5$ MeV and $\nu=0$ through 5.

the nearest $(\alpha,\alpha_0)$ resonances; so these are probably new states.

Of the six natural parity resonances observed in both $(p,\alpha_0)$ and $(p,\alpha_1)$ reported in recent $^{23}$Na+$p$ work [8] (that are in our energy range) we find relatively little agreement with our experiment (see Table II). However, the narrow 14.227 MeV ($4^+$, $\Gamma_{\alpha_0}=2.0$ keV, $\Gamma_{\alpha_1}=2.0$ keV) resonance observed in Ref. [8] probably corresponds with our narrow ($\Gamma<13$ keV) 14.238 MeV ($L=2$) state. Their 15.40 MeV ($\Gamma_{lab}=22\pm6$ keV) state might correspond to our 15.365 MeV ($4^+$, $\Gamma_{lab}=25$ keV) state, which corresponds to a doublet seen in our $(\alpha,\alpha_0)$ work [1]. A comparison of our results with those of Ref. [8] is found in Table II.

Work on the $^{20}$Ne$(\alpha,\gamma)^{24}$Mg reaction [9] led to the observation of narrow states at $E_\alpha=5.720$ and 5.796 MeV ($\pm5$ keV). These correspond in energy to the first and second states in Table I. In $^{20}$Ne$(\alpha,\gamma_0)^{24}$Mg [10] a $1^-$ level was observed at $E_\alpha=6.60$ MeV, perhaps corresponding to a possible $L=(1,2)$ level at $E_\alpha=6.54$ MeV seen in the present work, though, more likely, it is the $4^+$

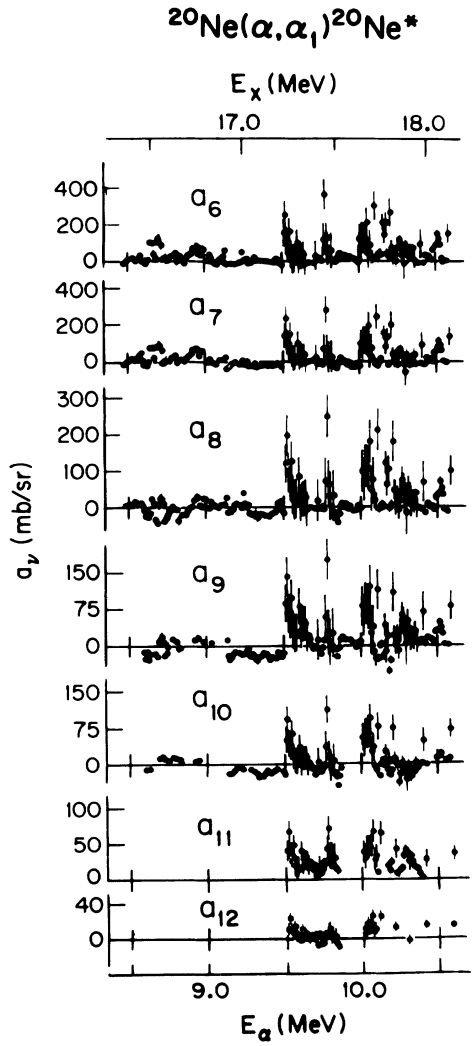


FIG. 6. As in Fig. 5 for $\nu=6$ through 12.

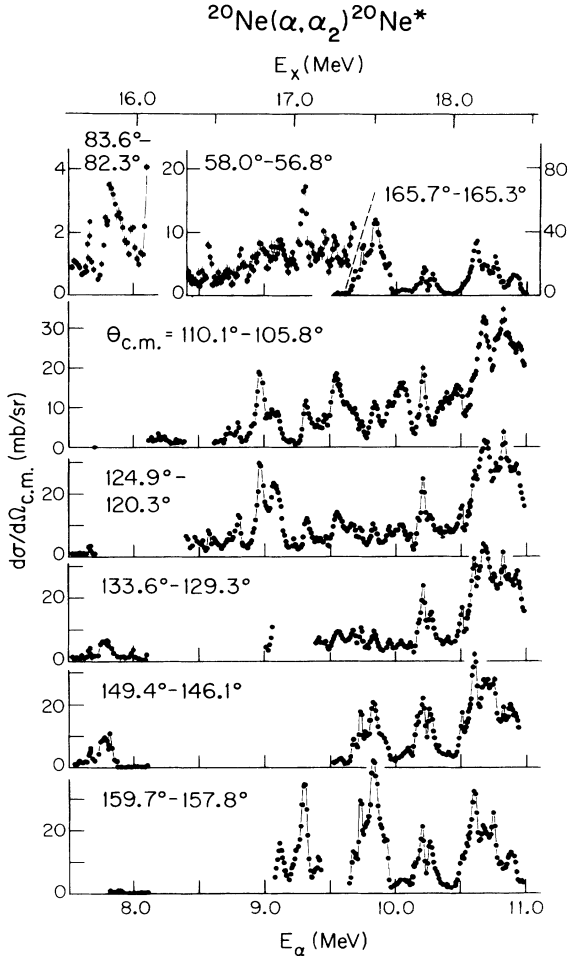


FIG. 7. Excitation functions at selected angles for inelastic $\alpha$ scattering to the second excited state of $^{20}$Ne. The line segments are a guide to the eye in regions of sharp structure.

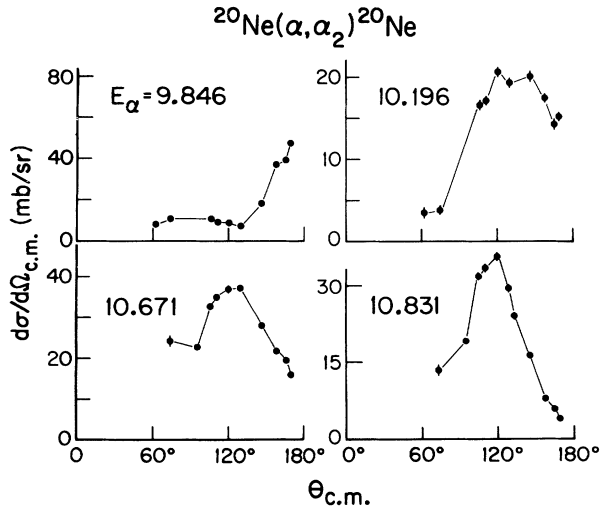


FIG. 8. Selected angular distributions for the $^{20}$Ne$(\alpha,\alpha_2)^{20}$Ne* reaction. The lines are merely a guide to the eye. The energies are in MeV.

TABLE II. Resonances in $^{24}$Mg deduced from the present work compared to natural parity states observed in at least one alpha channel in Ref. [8]. The first through third columns are from Table I. The fourth column is the preferred $J^\pi$ based on the present work and the assumed corresponding level from Ref. [1], with other possibilities from the present work shown in parentheses.

| $(\alpha,\alpha_1)$ resonances (present work) | | | | $(p,\alpha_i)$ resonances (Ref. [8]) | | | |
|---|---|---|---|---|---|---|---|
| $E_x$ (MeV) | $\Gamma_{c.m.}$ (keV) | $L$ | $J^\pi$ | $E_x$ (MeV) | $\Gamma_{lab}$ (keV) | $J^\pi$ | $(p,\alpha_i)$ |
| 14.072 | 21 | 2 | $2^+,4^+$ | 14.080 | 1.25 | $2^+$ | $\alpha_0$ |
| | | | | 14.088 | 30 | $1^-$ | $\alpha_0$ |
| | | | | 14.096 | 22.5 | $3^-$ | $\alpha_1$ |
| 14.134 | ≤13 | 2 | $4^+(2^+)$ | 14.1275 | 2.2 | $2^+$ | $\alpha_0,\alpha_1$ |
| 14.238 | ≤13 | 2 | $4^+(2^+)$ | 14.227 | 5.5 | $4^+$ | $\alpha_0,\alpha_1$ |
| 14.362 | ≤13 | 2 | $4^+(2^+)$ | 14.3625 | 15.7 | $(4)^+$ | $\alpha_0$ |
| 14.424 | 42 | 2 | $4^+(2^+)$ | 14.414 | 5 | $(4^+)$ | $\alpha_0$ |
| | | | | 14.415 | 1.5 | $3^-$ | $\alpha_0$ |
| | | | | 14.458 | 10 | $2^+$ | $\alpha_0$ |
| 14.601 | ≤13 | (3) | $5^-,(3^-)$ | 14.604 | 8 | $(1^-)$ | $\alpha_1$ |
| 14.661 | ≤15 | 4 | $6^+(4^+)$ | 14.653 | 72 | $(4^+)$ | $\alpha_0,\alpha_1$ |
| | | | | 14.663 | 3.4 | $3^-$ | $\alpha_0$ |
| 14.705 | 21 | 3 | $5^-(3^-)$ | 14.695 | 16 | $(2)^+$ | $\alpha_1$ |
| | | | | 14.705 | 14 | $1^-$ | $\alpha_0$ |
| 14.76 | ≤21 | (1,2) | $4^+(1^-,2^+,3^-)$ | 14.778 | 55 | $1^-$ | $\alpha_0$ |
| 14.970 | ≤13 | 3 | $5^-(3^-)$ | 14.967 | 10±3 | $^{nat}J$ | $\alpha_0$ |
| 15.209 | 33 | 3(4) | $5^-(3^-,4^+,6^+)$ | 15.18 | 40 | $2^+$ | $\alpha_0,\alpha_1$ |
| 15.365 | 25 | 2(3) | $4^+(2^+,3^-,5^-)$ | 15.40 | 22±6 | $^{nat}J$ | $\alpha_0,\alpha_1$ |
| 15.510 | 21 | (5,6) | $6^+(5^-,7^-,8^+)$ | 15.527 | <10 | | $\alpha_1$ |

level reported in the $(\alpha,\alpha_0)$ work [1]. Newer data on the $^{20}$Ne$(\alpha,\gamma)^{24}$Mg* reaction [11] also observed narrow levels at $E_\alpha=5.720$ and 5.799 MeV, corresponding to the resonances seen in Ref. [9], but ruling out a correspondence with our broader ($\Gamma=21$ keV) 5.715 MeV state.

Levels reported in $^{20}$Ne$(\alpha,\alpha'\gamma_{1.63})^{20}$Ne [11] at $E_\alpha=5.715$ MeV±5 keV ($\Gamma=24\pm5$ keV), 5.801 MeV ($\Gamma=6.2\pm0.7$ keV), and 5.913 MeV±5 keV ($\Gamma=11.3\pm1.4$ keV) correspond well to our first three $(\alpha,\alpha_1)$ levels. A broad unlabeled resonance is also apparent in their [11] data and is consistent with our broad 14.32 MeV ($\Gamma\simeq167$ keV) state. Additional $^{20}$Ne$(\alpha,\gamma)$ studies [12] using $\gamma$-ray angular distributions and decay schemes report a $(2,4)^+$ assignment for a $E_x=14.10$ MeV state which would seem to match our first state except for the $\Gamma=1.4\pm0.4$ keV measured by Ref. [11]. Reference [12] also limited a $\Gamma=1.8\pm0.4$ keV, 14.146 MeV state to $4^+,(3^-,5^-)$. All these parameters are consistent with our second level; see Table I.

Data on the $^{20}$Ne$(\alpha,\alpha'\gamma_{1.63})^{20}$Ne reaction were also reported up to $E_\alpha=6.08$ MeV in Ref. [13]. Their [13] yield curve (their Fig. 2) corresponds nicely with our $\sigma_T$ at the low end of our energy range (see Fig. 3, top panel), indicating that their peaks labeled $Y$, $\alpha$, $\gamma$, and $\delta$ correspond to our first four states (in Table I).

## ACKNOWLEDGMENTS

The author thanks Hugh T. Richards for guidance and comments. Many thanks to Rudy Abegg for his assistance and advice. Also, thanks to Dan Steck, Steve Riedhauser, James Billen, and Lawrence Ames for assistance during data collection. This work was supported in part by the United States Department of Energy and the National Science Foundation.

[1] R. Abegg and C. A. Davis, Phys. Rev. C **43**, 2523 (1991).
[2] P. M. Endt, Nucl. Phys. **A521**, (1990); P. M. Endt and C. van der Leun, *ibid.* **A310**, 1 (1978); **A214**, 1 (1973).
[3] C. A. Davis, Phys. Rev. C **24**, 1891 (1981).
[4] See AIP document No. PAPS-PRVCA-45-2693-117 for 117 pages of differential cross sections and Legendre polynomial expansion coefficients (including total cross sections). Order by PAPS number and journal reference from American Institute of Physics, Physics Auxiliary Publication Service, 335 East 45th Street, New York, NY 10017. The price is $1.50 for microfiche or $5 for photocopies. Make checks payable to the American Institute of Physics.
[5] C. A. Davis, Ph.D thesis, University of Wisconsin, 1969. Available through University Microfilms, Inc., Ann Arbor, Michigan.
[6] E. Eisner and R. G. Sachs, Phys. Rev. **72**, 680 (1947).
[7] L. Wolfenstein and R. G. Sachs, Phys. Rev. **73**, 528 (1948).
[8] J. R. Vanhoy, E. G. Bilpuch, C. R. Westerfeldt, and G. E.

Mitchell, Phys. Rev. C **36**, 920 (1987).
[9] G. J. Highland and T. T. Thwaites, Nucl. Phys. **A109**, 163 (1968).
[10] E. Kuhlmann, E. Ventura, J. R. Calarco, D. G. Mavis, and S. S. Hanna, Phys. Rev. C **11**, 1525 (1975).
[11] L. K. Fifield, M. J. Hurst, T. J. M. Symons, F. Watt, C. H. Zimmerman, and K. W. Allen, Nucl. Phys. **A309**, 77 (1978).
[12] L. K. Fifield, E. F. Garman, M. J. Hurst, T. J. M. Symons, F. Watt, C. H. Zimmerman, and K. W. Allen, Nucl. Phys. **A322**, 1 (1979).
[13] R. H. Spear and I. F. Wright, Aust. J. Phys. **21**, 307 (1968).